Cell Surface Expression of Receptor Protein Tyrosine Phosphatase RPTPμ Is Regulated by Cell–Cell Contact

Martijn F. B. G. Gebbink, Gerben C. M. Zondag, Gregory M. Koningstein, Elles Feiken, Richard W. Wubbolts, and Wouter H. Moolenaar

Division of Cellular Biochemistry, The Netherlands Cancer Institute, 1066 CX Amsterdam, The Netherlands

Abstract. RPTPμ is a transmembrane protein tyrosine phosphatase with an adhesion molecule-like ectodomain. It has recently been shown that RPTPμ mediates homophilic interactions when expressed in insect cells. In this study, we have examined how RPTPμ may function as a cell contact receptor in mink lung epithelial cells, which express RPTPμ endogenously, as well as in transfected 3T3 cells. We find that RPTPμ has a relatively short half-life (3–4 hours) and undergoes posttranslational cleavage into two noncovalently associated subunits, with both cleaved and uncleaved molecules being present on the cell surface (roughly at a 1:1 ratio); shedding of the ectodomain subunit is observed in exponentially growing cells. Immunofluorescence analysis reveals that surface expression of RPTPμ is restricted to regions of tight cell–cell contact. RPTPμ surface expression increases significantly with increasing cell density. This density-induced upregulation of RPTPμ is independent of its catalytic activity and is also observed when transcription is driven by a constitutive promoter, indicating that modulation of RPTPμ surface expression occurs posttranscriptionally. Based on our results, we propose the following model of RPTPμ function: In the absence of cell–cell contact, newly synthesized RPTPμ molecules are rapidly cleared from the cell surface. Cell–cell contact causes RPTPμ to be trapped at the surface through homophilic binding, resulting in accumulation of RPTPμ at intercellular contact regions. This contact-induced clustering of RPTPμ may then lead to tyrosine dephosphorylation of intracellular substrates at cell–cell contacts.

RECEPTOR-like protein tyrosine phosphatases (receptor PTPs)[1] represent a new family of transmembrane proteins that are thought to transduce external signals by dephosphorylating phosphotyrosine residues on intracellular substrates (for review see Walton and Dixon, 1993). Although the receptor PTPs are growing in number and diversity, little is known about the nature of their extracellular ligands and their normal intracellular activities. It is also unknown where at the cell surface receptor PTPs are localized and how delivery and localization to the cell surface is regulated.

We have recently cloned and characterized a mammalian receptor PTP, termed RPTPμ, which has an ectodomain similar to both the Ig-like and fibronectin type III–like domains of cell adhesion molecules (Gebbink et al., 1991). We and others have shown that RPTPμ can mediate cell–cell adhesion when expressed in nonadherent insect cells (Gebbink et al., 1993*a*; Brady-Kalnay et al., 1993). RPTPμ-mediated cell adhesion is calcium independent and does not require a functional intracellular catalytic domain. Cell–cell adhesion can also be mediated by a closely related receptor PTP, termed RPTPκ (Jiang et al., 1993), but despite their structural resemblance, RPTPμ and RPTPκ fail to undergo heterophilic interactions (Zondag et al., 1995). These results strongly suggest that RPTPμ and related receptor PTPs serve a role in cell–cell recognition and signaling. In general, cell–cell signaling is fundamental to embryonic development, tissue renewal, and tumor suppression. In particular, by coupling cell–cell interaction to the regulation of protein tyrosine phosphorylation, RPTPμ might transduce signals involved in contact-mediated growth inhibition and differentiation. However, experimental data on RPTPμ functioning within a monolayer of mammalian cells are still lacking.

To examine how RPTPμ may function in contact-mediated signaling, we have studied the mechanisms that control the disposition and distribution of RPTPμ at the surface of mammalian cells as a function of cell–cell contact. Through biochemical and immunofluorescence analysis of mink lung epithelial cells, which express RPTPμ endoge-

Address all correspondence to W. H. Moolenaar, Div. of Cellular Biochemistry, The Netherlands Cancer Institute, Plesmanlaan 121, 1066 CX Amsterdam, The Netherlands. Tel.: (0) 20-512 1971. Fax: (0) 20-512 1989.

Both Martijn F. B. G. Gebbink and Gerben C. M. Zondag contributed equally to this work.

1. *Abbreviations used in this paper*: ExG, chimeric construct of human RPTPμ; ExJ, XJ, truncated human RPTPμ; GST, glutathione *S*-transferase; PTP, protein tyrosine phosphatase.

nously, and 3T3 cells stably transfected with wild-type or mutant RPTPμ cDNAs, we show that surface expression of RPTPμ increases with cell density and is regulated by cell–cell contact. The results lead to a model in which homophilic binding causes newly synthesized RPTPμ to accumulate at regions of cell–cell contact. The cell biological implications of this model are discussed.

Materials and Methods

Cells

Mink lung epithelial cells (CCL64; American Type Culture Collection, Rockville, MD) mouse NIH-3T3 cells (clone 2.2; Livney et al., 1987), monkey COS cells, Rat-1 fibroblasts, human MelJuso melanoma cells, human mammary carcinoma (Lucy), and mouse N1E-N115 neuroblastoma cells were cultured in DME supplemented with 10% FCS. Porcine aortic endothelial (PAE) cells (Miyazono et al., 1988) were kindly provided by C. H. Heldin (Ludwig Institute, Uppsala, Sweden) and grown in Ham's F-10 medium (Life Technologies, Inc., Grand Island, NY) with 10% FCS. Rat adrenal pheochromocytoma (PC12) cells were grown in DME with 10% FCS and 5% horse serum. Human umbilical vein endothelial cells were isolated by trypsin digestion of umbilical veins and cultured on fibronectin-coated plates in RPMI1640I and M199 media (1:1 mixture) with 20% human serum. SP2/0 myeloma cells and hybridomas were grown in Iscove's medium supplemented with 10% FCS. Insect Sf9 cells were grown in Grace's medium.

cDNA Constructs

The generation of cDNAs encoding either the full-length human RPTPμ or a truncated form (termed either ExJ or XJ) lacking both phosphatase domains has been described previously (Gebbink et al., 1993*a*). A chimeric construct (ExG) containing the extracellular domain of RPTPμ fused COOH terminally to glutathione *S*-transferase (GST) was generated in a two-step polymerase chain reaction procedure. First, GST was amplified using pGEX (Smith and Johnson, 1988) as template using oligonucleotides 5′-GACCATACAGTTAAAATGTCCCCTATACTAGGT-3′ and 5′-CCCCTCTAGAT-CATTTTGGAGGATGGTCGCCA-3′; a fragment of RPTPμ was amplified with oligonucleotides 5′-CTCAAT-GTCTACGTGAAGGCT3′ and 5′-TAGTATAGGGGACATTTTAA-CTGTATGGTCTGT-3′. Both overlapping fragments were purified on gel and mixed. Next, a fusion construct was amplified using oligonucleotides 5′-GACCATACAGTTAAAATGTCCCCTATACTAGGT-3′ and 5′-CTC-AATGTCTACGTGAAGGCT-3′ and recloned as a NdeI(bp 1537)-XbaI fragment into a Bluescript vector that contained the remaining NH_2-terminal RPTPμ coding sequences. The resulting cDNA construct encodes the entire extracellular domain of RPTPμ and GST. This construct was subcloned into the eukaryotic expression vector pMT2.

Antibodies

To generate mAbs against the RPTPμ ectodomain, we sought to produce large amounts of a secreted ectodomain fusion protein in transfected 3T3 cells, rather than in *Escherichia coli.* The fusion construct, termed ExG, encodes the entire ectodomain of the human RPTPμ molecule (aa 1-742; Gebbink et al., 1991) fused COOH terminally to GST (Fig. 1 *A*). NIH-3T3 cells transfected with this construct secrete the ExG protein into the medium, from which it was readily purified with glutathione beads (yield: ~1 mg/liter culture medium; Fig. 1 *B*) and then used for immunizing mice. Mice were injected intraperitoneally three times with ~50 μg protein bound to glutathione Sepharose beads (Pharmacia, Uppsala, Sweden) at 2 wk intervals. 6 wk after the last immunization, one mouse was selected and boosted intravenously with ExG, eluted from the Sepharose beads. After 3 d, the mouse was killed and spleen cells were fused with SP2/0 myeloma cells to generate hybridoma cell lines according to Harlow and Lane (1988). Hybridoma supernatants were tested by ELISA and FACS® analysis. Supernatants were tested for recognizing human RPTPμ expressed on the surface of transfected 3T3 cells, which lack endogenous RPTPμ. Positive hybridomas were selected and cloned. Fig. 1 *C* shows a representative FACS® analysis of RPTPμ-expressing cells using mAb 3D7; this mAb recognizes not only human but also rodent RPTPμ (endogenously expressed in mink and rat cells; see Fig. 1 *C* and Results). Six out of seven mAbs precipitate a protein of approximately 195 kD (Fig. 1 *D*, lanes 2–8; these mAbs also detect a cleavage product of ~100 kD, as will be detailed under Results).

Antiserum 37 (Ab37) raised against a synthetic peptide corresponding to the COOH terminus of RPTPμ has been described previously (Gebbink et al., 1991). Mouse mAb 3G4 (Ig2b/κ) was raised against the extracellular fibronectin type III repeats of human RPTPμ (Gebbink et al., 1993*a*). An anti-GST mAb, 2F3, was obtained during the same screen. mAb 108, recognizing the extracellular domain of the EGF receptor, rabbit polyclonal anti-EGFR COOH terminal antiserum and anti-PLCγ (Margolis et al., 1989) were kindly provided by J. Schlessinger (New York University). Antidiacylglycerol kinase mAbs (Schaap et al., 1993) were kindly provided by D. Schaap (The Netherlands Cancer Institute). For immunoprecipiation of phosphotyrosine-containing proteins, 1 μg antiphosphotyrosine antibody PY20 (Affiniti Research Products Ltd., UK) was used per milligram of total protein. For antiphosphotyrosine immunoblots, antibody 4G10 (Upstate Biotechnology, Inc., Lake Placid, NY) was used.

Transient Expression in COS Cells and Insect Sf9 Cells

COS cells were transfected using the calcium phosphate precipitation method described by Gebbink et al. (1991). Insect Sf9 cells were infected with recombinant Ac-pVLhFL baculovirus (Gebbink et al., 1993*a*) for 24 h.

Stable Transfection of 3T3 Cells

Mouse NIH 3T3 cells (clone 2.2, which lacks endogenous EGF receptors; Livney et al., 1987) were cotransfected with the appropriate cDNA construct and a vector with the neomycin resistance gene (pSV2-neo; Spivak et al., 1984) using the calcium phosphate precipitation method. Stable transfectants were selected by G418 resistance (Gibco Life Technologies, Inc.). Single-cell subclones were generated by limited dilution.

Flow Cytometry

3T3 cells were washed with PBS and incubated for 10 min in PBS containing 0.5 mM EDTA and 0.02% (wt/vol) NaN_3. Strongly adherent mink lung cells were collected by incubation for 10 min with trypsin + EDTA containing 0.02% NaN_3. Cells were harvested by centrifugation and resuspended; 10^6 cells were used per staining. FACS® analysis was done by indirect immunofluorescence with fluorescein-conjugated goat anti–mouse $F(ab')_2$ (Zymed Laboratories, Inc., South San Francisco, CA) using a FACScan instrument (Becton Dickinson & Co., Mountain View, CA).

Metabolic Labeling

Cells grown in 10-cm dishes were washed twice with DME and then preincubated for 45 min in methionine-free minimal essential medium. Cells were labeled with 50 μCi/ml [^{35}S]methionine (Amersham International, Amersham, UK) for different time periods. Sf9 cells were labeled in methionine-free Grace's medium (Life Technologies, Inc.).

Cell Surface Iodination

Cells grown in 10-cm plates were washed three times with PBS and incubated for 15 min in 500 μl PBS with 10 μl lactoperoxidase (100 μg), 10 μl $Na^{125}I$ (1 mCi; Amersham) and 25 μl freshly prepared H_2O_2 (0.1% in PBS). After 7.5 min of incubation, fresh lactoperoxidase (10 μl) and H_2O_2 (25 μl) were added. Iodinated cells were lysed and RPTPμ precipitated with mAb 3D7 followed by SDS-PAGE analysis and autoradiography.

Immunoprecipitation and Immunoblotting

Cells were washed three times with ice-cold PBS and lysed in NP-40 lysis buffer (20 mM Tris-HCl, pH 7.5, 150 mM NaCl, 5 mM EDTA, 10% glycerol, 1% NP-40, 2 mM PMSF, 5 μg/ml leupeptin, 2.5 μg/ml aprotonin). After centrifugation, the supernatant was precleared with protein A–Sepharose (Pharmacia). When polyclonal antibody Ab37 was used, an equal volume of 2× BUSS buffer (1× BUSS: 150 mM NaCl, 10 mM NaH_2PO_4 pH 7.8, 1 mM DTT, 1.0% sodium deoxycholate, 0.5% SDS, and 1% NP-40) was added. Protein A–Sepharose preincubated with specific antibodies was added, and lysates were incubated for 2 h. Immune complexes were washed three times with lysis buffer, transferred to a new tube, and washed once again. Where indicated, the immunoprecipitates were incubated for 2 h with 3 U Endo F (Boehringer Mannheim, Mannheim, Germany) after boiling for 1 min in 20 μl Endo F digestion buffer (0.25 M NaAC, pH 6.1, 20 mM EDTA, 10 mM β-mercaptoethanol, 0.1% SDS), subsequent cool-

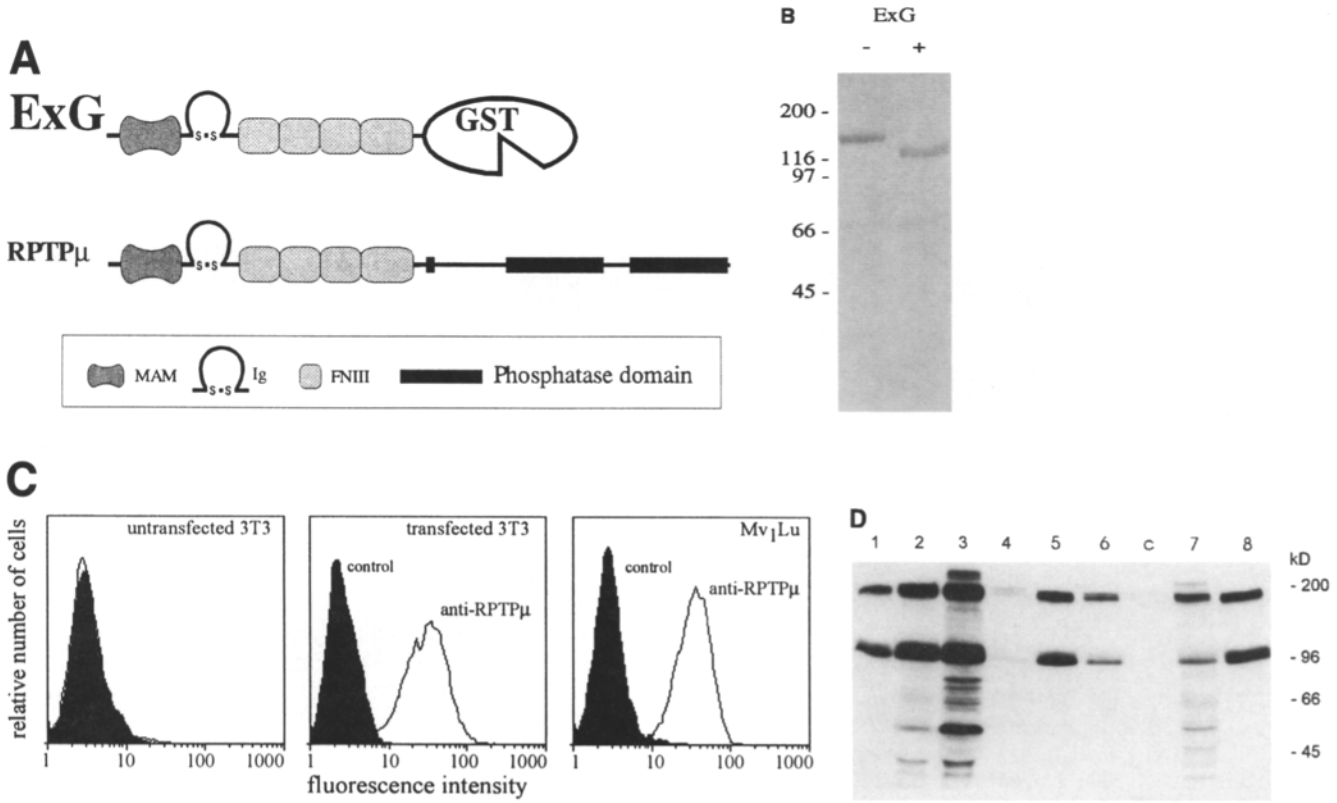

Figure 1. Generation and analysis of mAbs against the RPTPμ ectodomain. (*A*) Schematic representation of the RPTPμ–GST fusion construct (*ExG*) compared with full-length RPTPμ. MAM, represents the domain homologous to meprin, A5 and μ (Beckmann and Bork, 1993); Ig is the immunoglobulin-like domain; and FNIII is the fibronectin type III-like repeat. The amino acid sequence linking RPTPμ and GST is indicated. (*B*) SDS-PAGE analysis of ExG protein purified from conditioned medium from ExG-transfected 3T3 cells (Coomassie blue staining). Purified ExG protein was treated with Endo F as indicated. Molecular mass standards are in kilodaltons. (*C*) Flow cytometric analysis of cell surface expression on untransfected 3T3, stably transfected 3T3[FL], and mink lung cell (Mv_1Lu) cultures. Cells were harvested and stained with anti-RPTPμ mAb (3D7) or control antibody (anti-GST mAb 2F3). (*D*) SDS-PAGE analysis of anti-RPTPμ immunoprecipitates. Lysates from 3T3[FL] cells labeled with [^{35}S]methionine for 2 h were precipitated with polyclonal COOH-terminal antipeptide antibody 37 (lane *1*), control antibody (anti-GST mAb 2F3; lane *C*), or with the following anti-RPTPμ mAbs: lane *2*, 4B7 (isotype: IgG2a/κ); lane *3*, 2G1 (IgG2a/κ), lane *4*, 2D7 (IgG1/κ); lane *5*, 3D7 (IgG2a/κ); lane *6*, 1E1 (IgG1/λ); lane *7*, 1D9 (IgG2b/κ); and lane *8*, 2C10 (IgG2b/κ). It is seen that mAbs 2D7 (lane *4*) and 1E1 (lane *6*) precipitate RPTPμ less efficiently (probably due to the low affinity of these IgG1 isotypes for protein A, rather than a lower affinity for RPTPμ, since both mAbs work well in FACS® analysis; not shown). mAb 2G1 (lane *3*) is seen to be less specific. The mAbs precipitate both the uncleaved form of RPTPμ (200 kD) as well as a cleaved form (100-kD doublet).

ing, and addition of 1 μl 20% NP-40. Alternatively, where indicated, the immunoprecipitates were incubated for 12 h with 2 U Endo H (Boehringer Mannheim) after boiling for 1 min in 20 μl Endo H digestion buffer (50 mM Na-citrate, pH 5.5, 0.2% SDS, 20 mM EDTA, 10 mM β-mercaptoethanol, 0.1% SDS). The reactions were stopped by boiling the samples in SDS sample buffer for 5 min. Immunoprecipitates were analyzed on 7.5% SDS-PAGE gels followed by autoradiography or immunoblotting. Immunoblots were probed with specific antibodies and developed using chemiluminescence (ECL; Amersham).

Immunofluorescence Microscopy

RPTPμ-expressing cells were grown on glass coverslips, fixed in PBS containing 4% paraformaldehyde, and incubated with mAb 3D7 followed by fluorescent staining using FITC-conjugated goat anti-mouse $F(ab')_2$. RPTPμ staining was analyzed using a confocal microscope (model MRC-600; Bio-Rad Laboratories, Richmond, CA).

Results

Endogenous Expression of RPTPμ

Little is known about the expression pattern of the RPTPμ protein; the highest mRNA levels have been found in murine lung, heart, and brain tissue (Gebbink et al., 1991). As shown in Fig. 2, immunoprecipitation and immunoblot experiments reveal that RPTPμ is expressed in many different cell types, including human and porcine vascular endothelial cells, human mammary carcinoma and melanoma cells, as well as in mink lung epithelial cells and Rat-1 fibroblasts, but not in NIH-3T3 cells, PC12 pheochromocytoma cells, nor in N1E-115 neuroblastoma cells. The highest endogenous expression is observed in mink lung epithelial cells; these cells express about half the levels found in stably transfected NIH-3T3 fibroblasts.

Biosynthesis and Processing of RPTPμ: Two-subunit Structure and Shedding of the Ectodomain

Virtually nothing is known about the biosynthesis of RPTPμ. We used mink lung epithelial cells and transfected 3T3 fibroblasts for biosynthesis analysis because these cells show the highest expression levels. As shown in Fig. 3 *A*, a COOH-terminal antibody precipitates not only the mature 195-kD RPTPμ protein but also a proteolytic product of RPTPμ (100-kD doublet). Similar RPTPμ pro-

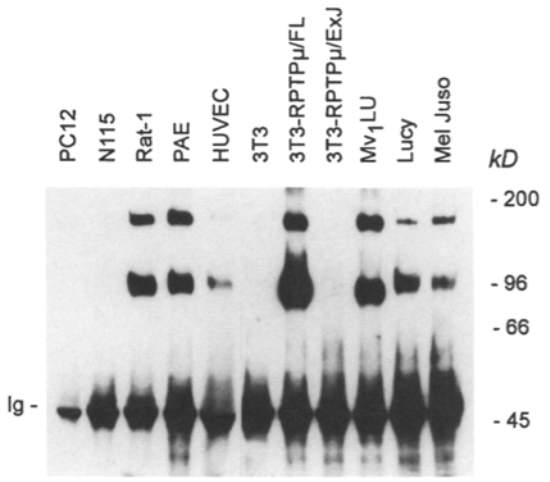

Figure 2. Expression of RPTPμ in various cell lines. RPTPμ was immunoprecipitated from 1 mg total protein using mAb 3D7 and analyzed by immunoblotting using anti–COOH-terminal Ab 37. The following cells were analyzed: PC12, rat adrenal pheochromocytoma; N115, mouse neuroblastoma; Rat-1, rat fibroblast; PAE, porcine aortic endothelial cells; HUVEC, human umbilical vein endothelial cells; 3T3, mouse NIH-3T3 fibroblasts; 3T3-RPTPμ/FL, 3T3 cells (3T3[FL] transfected with full-length RPTPμ cDNA; 3T3-RPTPμ/ExJ, 3T3 cells (3T3[XJ]) transfected with truncated RPTPμ cDNA, lacking the entire catalytic domain (and thus not recognized by COOH-terminal Ab 37); Mv_1LU, mink lung cells; Lucy, human ovarium carcinoma; Mel-Juso, human melanoma. Both mAb 3D7 and Ab37 recognize the mouse homolog of RPTPμ, as determined by transient transfection of the mouse cDNA in COS cells (not shown). Note that, in addition to the 195-kD full-length RPTPμ protein, the 100-kD proteolytic product is also detected in all cell types tested.

tein products have recently been detected by immunoblot analysis (Brady-Kalnay and Tonks, 1994). Treatment of the immunoprecipitates with Endo F, which removes N-linked carbohydrates, reduces the size of the full-length protein to 160 kD, whereas the cleaved products migrate around 93 and 68 kD. From these results, we infer that the NH_2-terminal 100-kD fragment is exclusively extracellular, whereas the COOH-terminal component comprises a small extracellular segment (containing two glycosylation sites), the transmembrane region and the intracellular domains. We also conclude that both subunits remain associated during cell lysis.

RPTPμ cleavage is also observed in transfected 3T3 cells (Fig. 1 *D*), but not in transiently transfected COS cells nor in baculovirus-infected Sf9 cells (Fig. 3 *A*). No cleavage is observed in the ExG fusion protein lacking the transmembrane region (Fig. 1 *B*), indicating that membrane anchoring is required for cleavage. Taken together, our results support an RPTPμ cleavage scheme as illustrated in Fig. 3 *B*. A similar cleavage pattern has also been proposed for two other receptor PTPs, namely LAR (Streuli et al., 1992; Yu et al., 1992) and RPTPκ (Jiang et al., 1993); the cellular protease(s) responsible remain(s) to be identified.

SDS-PAGE analysis of immunoprecipitated RPTPμ from surface-iodinated mink cells reveals that both the cleaved and full-length forms of RPTPμ are present on the cell surface, at an estimated ratio of approximately 1:1 (Fig. 3 *C*). A similar ratio of cleaved/uncleaved RPTPμ molecules was found in the 3T3 transfectants, as shown below (see Fig. 5 *B*).

The RPTPμ cleavage scheme shown in Fig. 3 *B* immediately suggests that the NH_2-terminal cleavage product, comprising almost the entire ectodomain, may be released into the extracellular environment. To test this possibility, conditioned medium and total cell lysates from transfected 3T3 cells were analyzed by immunoprecipitation. Fig. 3 *D* shows that, indeed, the 100-kD ectodomain fragment can be immunoprecipitated from the medium of exponentially growing 3T3 transfectants, but not from medium of non-transfected control cells; in total cell lysates, the same antibody precipitates both uncleaved RPTPμ and the cleaved ectodomain (Fig. 3 *D*).

The delivery of newly synthesized RPTPμ to the cell surface and its processing was further examined by [^{35}S]methionine pulse–chase analysis in combination with Endo H digestions. During a 30-min labeling pulse, no cleavage is observed (Fig. 4; $t = 0$). When pulse-labeled cells are subsequently chased for various times, two cleavage products of ~100 kD begin to appear simultaneously. Furthermore, it is seen that newly synthesized RPTPμ becomes fully resistant to Endo H treatment, which occurs during intracellular transport through the Golgi apparatus. The proteolytic products are fully Endo H resistant, indicating that cleavage occurs after transit through the Golgi apparatus. It is also seen that at chase periods >2 h, when Endo H–sensitive RPTPμ is hardly detectable, not all RPTPμ protein has undergone cleavage. It thus appears that both cleaved and uncleaved RPTPμ molecules can be transported to the cell surface. We estimate the half-life of RPTPμ in 3T3 and mink cells (Fig. 4 *B*, *middle panel*) at ~3–4 h; for comparison, the estimated half-life of the EGF receptor in mink cells is >8 h (Fig. 4 *B*, *right panel*).

RPTPμ Biosynthesis and Processing Is Independent of Catalytic Activity

We examined whether the catalytic activity of RPTPμ is important for its biosynthesis and delivery to the cell surface. To this end, we performed [^{35}S]methionine pulse–chase analysis of 3T3 cells stably transfected with a truncated, membrane-anchored form of RPTPμ (termed ExJ or XJ), which lacks the entire catalytic region. As can be seen in Fig. 4 *B* (*left panel*), the biosynthesis of truncated RPTPμ, its proteolysis, and estimated half-life are very similar to what is observed with full-length RPTPμ. Thus, biosynthesis and intracellular transport of RPTPμ do not depend on its catalytic activity.

Localization of RPTPμ at Intercellular Contact Regions and RPTPμ Stabilization at the Cell Surface

Our previous work has shown that RPTPμ, when expressed in nonadhesive insect cells, has a uniform distribution along the plasma membrane (Gebbink et al., 1993*a*). However, the surface localization of RPTPμ (or any other receptor PTP) in mammalian cells has not been examined to date.

We analyzed RPTPμ expression by immunofluorescence microscopy using mAb 3D7, which is directed against

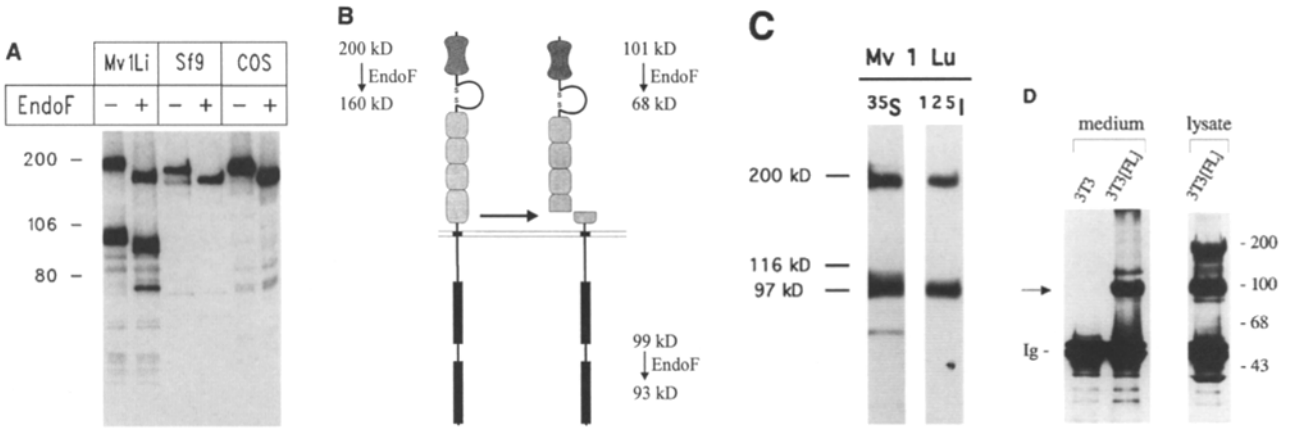

Figure 3. Processing of RPTPμ. (*A*) Mink lung cells (Mv_1Lu), transiently transfected COS cells, and recombinant baculovirus-infected Sf9 cells were labeled with [^{35}S]methionine (16 h) and RPTPμ was precipitated from cell lysates using anti–COOH-terminal Ab 37. Immunoprecipitates were split and treated with either Endo F or control buffer for 2 h followed by SDS-PAGE. Note that RPTPμ from mink lung cells migrates somewhat slower than RPTPμ from COS or Sf9 cells, probably due to more extensive glycosylation. The molecular mass of the protein before and after cleavage and Endo F treatment is indicated. The intensity of the 68-kD cleaved ectodomain is lower than that of the remaining COOH-terminal part, since the NH_2-terminal cleavage product contains only 7 methionine residues compared with the COOH-terminal part, which contains 28 residues. (*B*) Schematic representation of the presumed processing of RPTPμ. The arrow indicates the proteolytic cleavage site. (*C*) Cell surface expression of RPTPμ. Confluent mink lung cells (Mv_1Lu) were either metabolically labeled with [^{35}S]methionine for 16 h or surface-labeled with ^{125}I as indicated. RPTPμ was precipitated with anti–COOH-terminal Ab 37 and analyzed by SDS-PAGE (7.5% gel). (*D*) Shedding of the RPTPμ ectodomain. Immunoblot analysis of anti-RPTPμ (mAb 3D7) immunoprecipitates from medium derived from transfected and untransfected 3T3 cells, cultured for 24 h. The blot was probed with anti-RPTPμ mAb 3G4. The arrow indicates the cleaved ectodomain of RPTPμ. For comparison, RPTPμ was immunoprecipited from lysates of the same cells and analyzed on the same blot. Note that in this lysate uncleaved RPTPμ is present, indicating that the shed ectodomain is not derived from dead cells.

the RPTPμ ectodomain, in combination with a fluorescein-conjugated second antibody. Fig. 5 *A* shows that in stably transfected 3T3 cells, intense fluorescence is strictly confined to those regions where the membranes of two cells are directly apposed. A similar restricted localization pattern was observed between adjacent mink lung epithelial cells (results not shown). Note that RPTPμ staining is not detected anywhere else on the cell surface, nor in cells that lack physical contact with their neighbors (Fig. 5 *A*). These observations suggest that RPTPμ is trapped and becomes concentrated on the cell surface through homophilic binding initiated by cell–cell contact. Such a mechanism predicts that surface-disposed RPTPμ, when trapped through homophilic binding, becomes stabilized and has a prolonged half-life. To test this prediction, we monitored the fate of ^{125}I-labeled RPTPμ at the surface of transfected 3T3 cultures (having numerous cell–cell contacts). Fig. 5 *B* shows that, indeed, iodinated RPTPμ expressed at the surface is stable: even after periods of up to 4 h, the RPTPμ ectodomain iodination signal is not significantly attenuated. In [^{35}S]methionine pulse–chase experiments carried out at high cell densities, we found a relatively small increase in the estimated half-life of the total population of newly synthesized RPTPμ (results not shown). This result is not unexpected in view of RPTPμ's very restricted localization pattern, that is, only at cell contacts; thus, in monolayer cultures the bulk of surface-disposed RPTPμ will not undergo homophilic binding and will not become stable.

Another prediction of the very restricted localization of RPTPμ is that RPTPμ cell surface expression would be upregulated when cell contact increases, that is, at increasing cell density, as tested below.

RPTPμ Surface Expression Is Up-regulated by Cell–cell Contact

We examined RPTPμ surface expression in mink lung epithelial cells as a function of cell density by FACS® analysis. Sparse cultures with little or no intercellular contacts show relatively low surface expression (Fig. 6 *A*, micrograph *I* and Fig. 6 *B*). However, when cells are grown to near confluence, RPTPμ expression is increased about twofold (Fig. 6 *A*, micrograph *II*, and Fig. 6 *B*). A further increase in cell surface RPTPμ levels (about threefold) is observed when cells are highly confluent with maximal intercellular contacts (Fig. 6 *A*, micrograph *III*). This density-dependent expression pattern of RPTPμ is in marked contrast to that of the receptor for EGF, whose surface expression is significantly downregulated at high cell density (Fig. 6).

The above FACS® analysis was complemented and extended by immunoblotting experiments. The results confirm that RPTPμ expression is significantly upregulated in high-density cultures, whereas endogenous EGF receptor levels are decreased (Fig. 6). In control experiments, expression of an intracellular signaling enzyme (phospholipase C) is seen to be independent of cell density (Fig. 6 *C*, *left panel*).

We also examined cellular phosphotyrosine patterns as a function of cell density. Antiphosphotyrosine immunoprecipitations followed by immunoblotting with antiphosphotyrosine antibody reveal that in high-density cultures, where RPTPμ expression is maximal, phosphotyrosine levels are significantly reduced (Fig. 6 *C*, *right panel*). The major tyrosine-phosphorylated substrates migrate at an

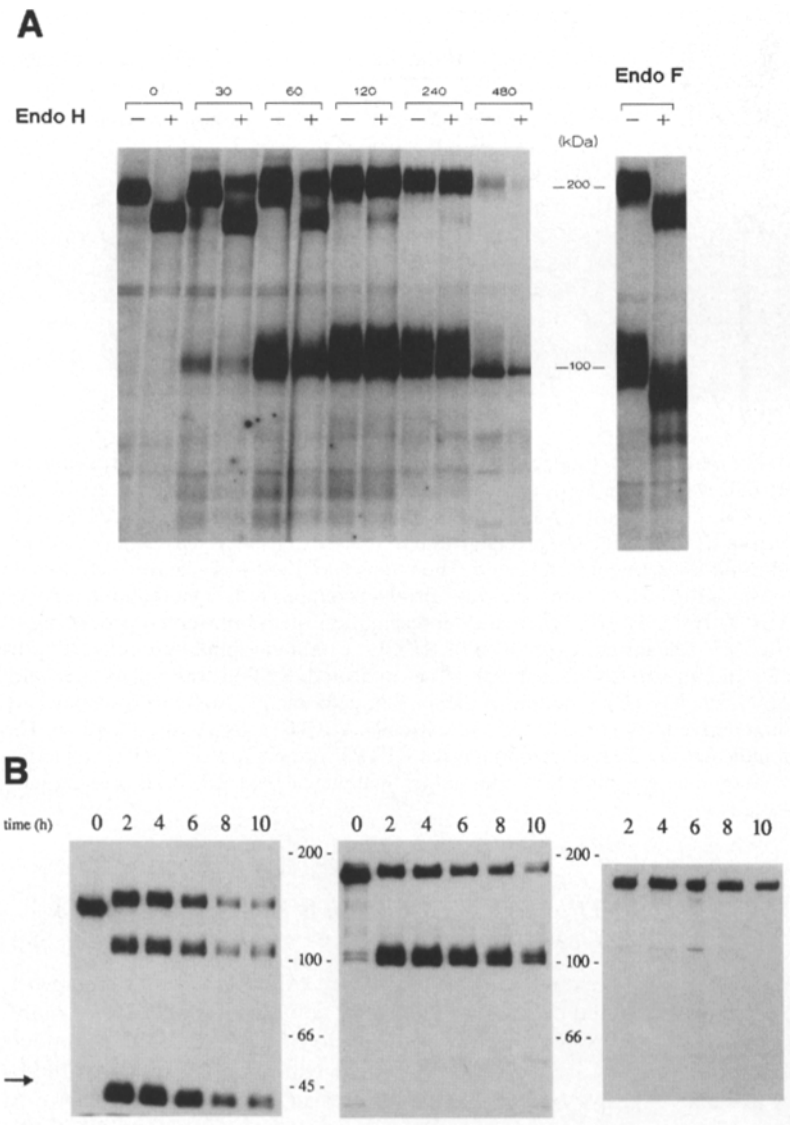

Figure. 4. Pulse-chase analysis of RPTPμ biosynthesis. (*A*) Transfected 3T3[FL] cells were pulse labeled with [^{35}S]methionine for 30 min and chased for the time periods indicated. After cell lysis, RPTPμ was precipitated using anti–COOH-terminal Ab 37. Immunoprecipitates were split, incubated either with or without Endo H, and analyzed by SDS-PAGE. For comparison, an additional plate of 3T3[FL] cells was labeled for 2 h in parallel, and precipitated RPTPμ was treated with or without Endo F, as indicated. (*B*) 3T3[XJ] transfectants (*left panel*) and mink lung cells (*middle* and *right panels*) were pulse labeled and chased as in *A*. After cell lysis, RPTPμ was precipitated using mAb 3D7 (*left* and *middle panels*). EGF receptor was subsequently precipitated from the mink cells using mAb 108 (*right panel*). In the 3T3[XJ] cells, truncated RPTPμ is cleaved into two subunits, the NH_2-terminal ectodomain of 100 kD and the remaining COOH-terminal portion of 40 kD (*arrow*), lacking the catalytic domains.

apparent molecular mass of 120–130 kD, but otherwise remain unidentified. From the same cell lysates, equal amounts of control protein (diacylglycerol kinase) were precipitated, indicating that the differences in RPTPμ, EGF receptor, and phosphotyrosine levels are physiological and not due to differences in immunoprecipitation conditions.

Density-dependent Expression of Full-Length and Truncated RPTPμ in 3T3 Transfectants

Having shown that surface expression of endogenous RPTPμ is upregulated at increasing cell density, we next examined how this regulation occurs. If enhanced RPTPμ surface expression would be induced at the transcriptional level, then it should not occur when RPTPμ expression is under the control of a constitutive promoter as in stably transfected 3T3 cells. Contrary to this prediction, transfected RPTPμ in 3T3 cells shows the same density-dependent expression pattern as endogenous RPTPμ in mink cells (Fig. 7). This implies that regulation of surface expression by cell–cell contact occurs posttranscriptionally. Thus, it appears that upregulation of RPTPμ surface expression is the direct result of increased cell–cell contact.

A similar density-dependent expression pattern was observed in 3T3 cells transfected with the truncated form of RPTPμ (ExJ), which lacks the entire catalytic domain (Fig. 7 *B*, *right panel*). This demonstrates that contact-induced surface expression of RPTPμ is regulated independently of its catalytic activity.

Discussion

Recent studies have shown that RPTPμ and a closely related receptor PTP, termed RPTPκ, can mediate homophilic but not heterophilic interactions when expressed in non-adhesive insect cells (Gebbink et al., 1993*a*; Brady-Kalnay et al., 1993; Sap et al., 1994; Zondag et al., 1995). This strongly suggests that these receptor PTPs play a role in cell recognition and subsequent cell–cell signaling. However, although the homophilic binding properties have been assessed in insect cell expression systems, very little experimental data are available on the cell biological aspects of RPTPμ function (and that of related receptor PTPs) in mammalian cells.

In this study, we have addressed the possible biological

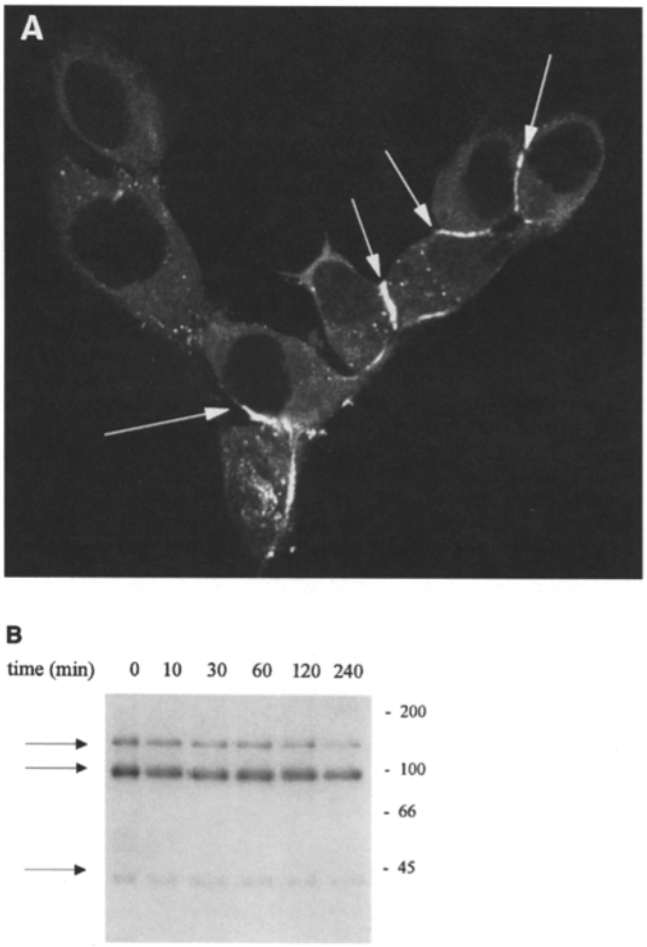

Figure 5. (*A*) RPTPμ expression in transfected 3T3 cells analyzed by indirect immunofluorescence using anti-RPTPμ mAb 3D7 and confocal microscopy. Note that RPTPμ localization is restricted to sites of close cell–cell contact (*arrows*). (*B*) Analysis of RPTPμ cell surface expression. Transfected 3T3 cells expressing the truncated form of RPTPμ (ExJ) were surface labeled with ^{125}I and then monitored for the indicated time periods. Cells were lysed and RPTPμ precipitated with mAb 3D7 followed by SDS-PAGE analysis and autoradiography. Arrows indicate the unprocessed (140 kD) and the proteolytically cleaved forms (100 and 40 kD, respectively).

function of RPTPμ as a cell contact receptor in mink lung epithelial cells and transfected 3T3 fibroblasts. Our major new findings can be summarized as follows: (*a*) Part of newly synthesized RPTPμ is proteolytically cleaved into two subunits; the NH_2-terminal subunit can undergo shedding from the cell surface; (*b*) RPTPμ has a relatively short half-life; (*c*) RPTPμ is highly concentrated at regions of close membrane apposition; (*d*) RPTPμ surface expression increases significantly with increasing cell density (whereas EGF receptor expression shows inverse correlation with cell density); and (*e*) density-dependent surface expression is regulated at a posttranscriptional level and is independent of RPTPμ catalytic activity. Based on these findings, we propose a model of how RPTPμ surface expression and biological activity is regulated by cell–cell contact, as will be discussed below.

RPTPμ Biosynthesis and Processing

During intracellular biosynthesis, RPTPμ can undergo posttranslational cleavage into two subunits, which apparently remain associated in a noncovalent manner. RPTPμ proteolysis was also reported in a recent study by Brady-Kalnay and Tonks (1994). Precisely how the two subunits are cleaved and hold together remains to be elucidated. A similar cleavage has been described for the related receptor PTPs LAR and RPTPκ, and also for Ng-CAM (Burgoon et al., 1991; Streuli et al., 1992; Yu et al., 1992; Jiang et al., 1993). Our results indicate, however, that both the full-length and cleaved forms of RPTPμ are present on the cell surface.

It is noteworthy that the NH_2-terminal subunit of RPTPμ, which comprises almost the entire ectodomain, is shed from the surface of exponentially growing cells. Shedding of the homophilic binding domain may serve to downregulate the function of RPTPμ as a cell contact receptor. If one assumes that full-length RPTPμ promotes growth inhibition through homophilic binding, then shedding of the ectodomain might be advantageous (and perhaps even necessary) for normal cell growth. An alternative or additional possibility is that the shedded ectodomain may function as a competitive inhibitor of RPTPμ-mediated homopilic interactions and thereby modulate growth behavior. Whatever the precise physiological function, it will be interesting to investigate whether RPTPμ shedding can be induced by growth factors. In this regard, it should be mentioned that shedding of the NH_2-terminal domain of another receptor PTP, LAR, is enhanced by protein kinase C–activating phorbol ester (Serra-Pages et al., 1994).

It appears that the half-life of RPTPμ is relatively short (3–4 h) as inferred from [^{35}S]methionine pulse–chase analysis. Furthermore, RPTPμ is rather difficult to radioiodinate in intact cells, suggesting that surface expression levels are relatively low. Taken together, these results support the notion that newly synthesized RPTPμ is rapidly internalized and degraded after being disposed at the cell surface.

RPTPμ as a Cell Contact Receptor

The finding that RPTPμ in mammalian cells is strictly localized to regions of intercellular contact (Fig. 5 *A*), rather than showing a uniform surface distribution as in insect cells (Gebbink et al., 1993*a*), provides direct support for the view that RPTPμ functions as a cell contact receptor mediating cell–cell signaling. Importantly, the ^{125}I-labeling experiments of Fig. 5 *B* indicate that RPTPμ expressed at the cell surface (i.e., the subpopulation concentrated at cell–cell contact regions) is quite stable when compared with the relatively short half-life of the total population of newly synthesized RPTPμ. Furthermore, we find that RPTPμ cell surface expression increases with cell density, that is, when there are more intercellular contacts. This density-dependent expression profile is observed not only in endogenously expressing mink lung epithelial cells but also in transfected 3T3 cells, where RPTPμ transcription is driven by a constitutive promoter. From these results we conclude that density-induced upregulation of RPTPμ surface expression occurs at the posttranscriptional level.

When this article was in preparation, Östman et al.

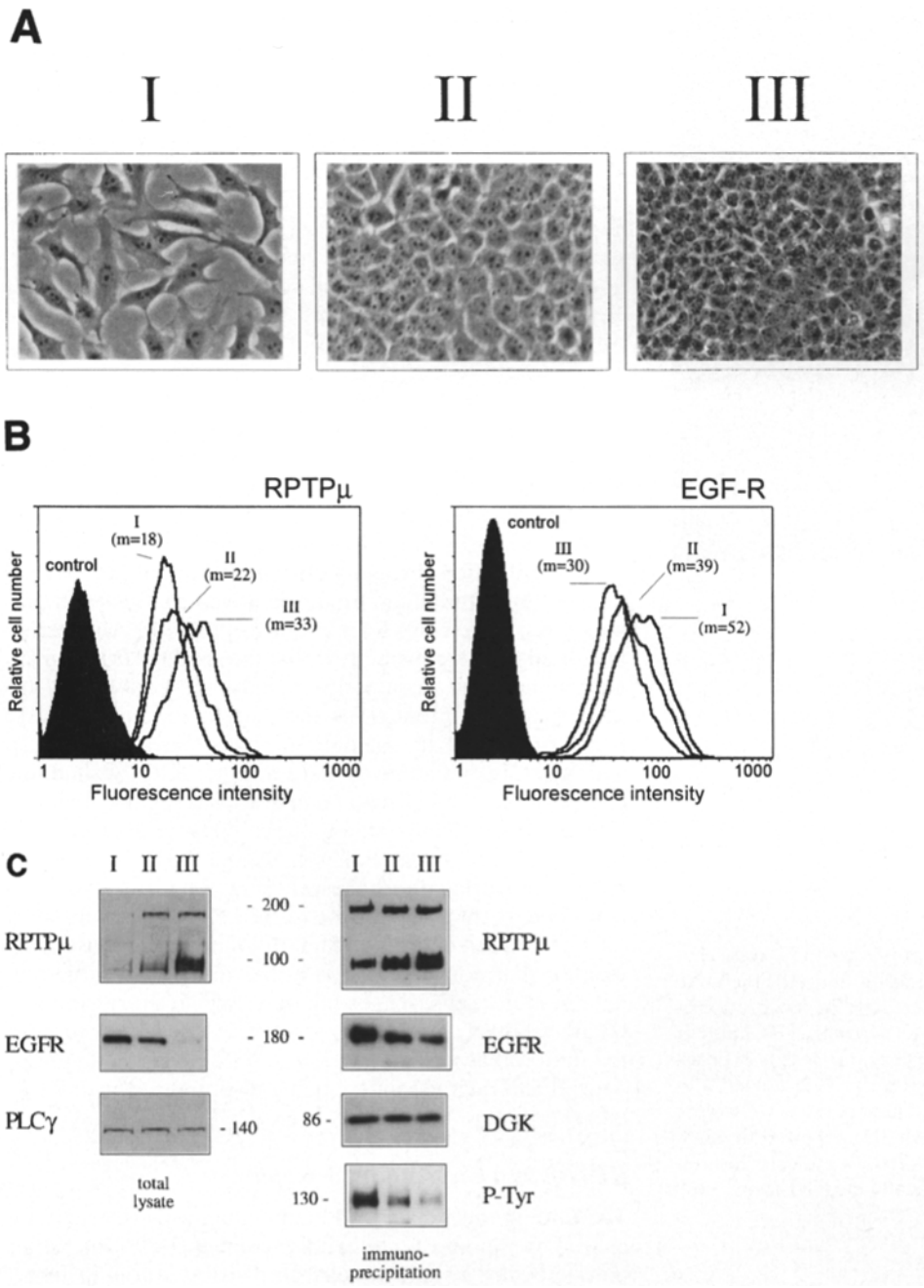

Figure 6. Regulation of RPTPμ cell surface expression by cell density. Mink lung cells were grown to low, medium, and high densities, and RPTPμ expression was examined. (*A*) Appearance of mink lung cells seeded at increasing densities, indicated with I, II, and III, respectively. (*B*) Flow cytometric analysis of RPTPμ cell surface expression on low (*I*), medium (*II*), and high (*III*) density cultures. Cells were stained using anti-RPTPμ mAb 3D7 (*left panel*) or anti-EGFR (*right panel*). Numbers represent arbitrary units of fluorescence. (*C*) *Left panel*, Expression of RPTPμ protein analyzed by immunoblotting. Equal amounts of total protein from mink lung epithelial cells were analyzed by SDS-PAGE followed by immunoblotting probed with anti-RPTPμ mAb 3G4. To control for equal amounts of protein loaded, the blot was reprobed with anti-PLCγ (*Control*). *Right panel*, Expression of RPTPμ and the EGF receptor was analyzed by immunoprecipitation with mAb 3D7 (anti-RPTPμ) or mAb 108 (anti-EGF receptor) followed by immunoblotting with mAb 3G4 (anti-RPTPμ) or a COOH-terminal anti-EGF receptor polyclonal antiserum. The effect of cell density on total protein tyrosine phosphorylation was analyzed by antiphosphotyrosine (PY20) immunoprecipitation and subsequent immunoblotting with antiphosphotyrosine antibody 4G10.

(1994) reported that expression of a newly cloned receptor PTP (termed DEP-1) is also enhanced with increasing cell density through an unknown mechanism; however, it remains to be seen whether this receptor PTP mediates cell–cell interactions.

The findings discussed here, together with our previous results, support the following model for the regulated expression of RPTPμ (Fig. 8). In sparse cultures without intercellular contacts, RPTPμ is nonfunctional: its surface expression levels are low because of rapid internalization and, furthermore, part of the surface-disposed RPTPμ molecules shed their ectodomain into the medium. Upon cell–cell contact, RPTPμ molecules on apposing cells recognize and bind each other in a homophilic manner, thereby preventing RPTPμ from being internalized. As a consequence, more and more RPTPμ molecules accumulate at regions of cell–cell contact, which then ultimately leads to local clustering of many RPTPμ molecules. Although all our results are consistent with surface-disposed RPTPμ being trapped at the cell surface through homophilic binding, we cannot rule out the possibility that increased RPTPμ biosynthesis may play a role as well.

Whatever the precise underlying mechanism, locally concentrated RPTPμ will promote net tyrosine dephosphorylation of as-yet-unidentified substrates at sites of cell–cell contact. It is important to note that in this model, cell–cell contact and subsequent clustering do not affect the basal activity of RPTPμ, which is already very high (at least in vitro; Gebbink et al., 1993*b*). Instead, contact-induced clustering of RPTPμ is thought to bring the cata-

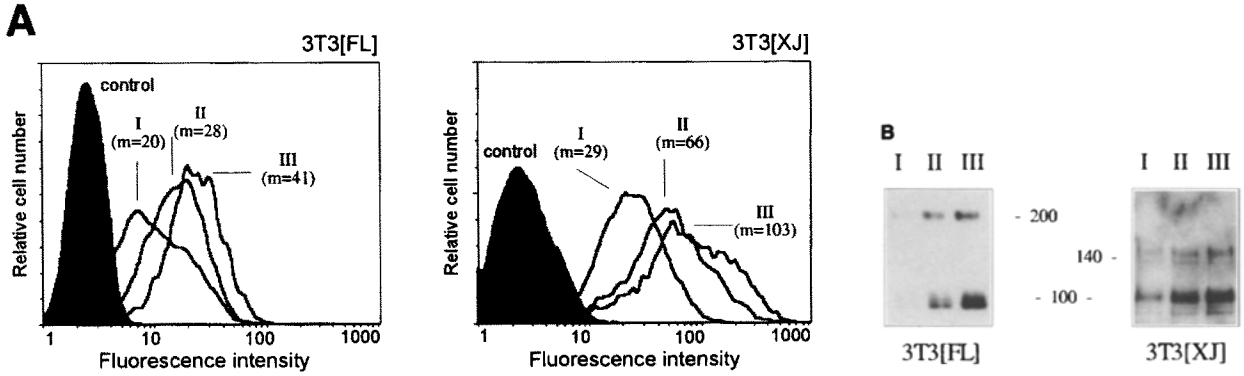

Figure 7. Regulation of RPTPμ cell surface expression by cell–cell contact in transfected 3T3 cells. Stably transfected 3T3[Fl] and 3T3[XJ] cells were grown to low, medium, and high densities, and RPTPμ expression was examined. (*A*) Cell surface expression as determined by FACS® analysis on low (*I*), medium (*II*), and high (*III*) density cell cultures. Cells were stained using anti-RPTPμ mAb 3D7. Numbers represent arbitrary units of fluorescence. (*B*) Expression of RPTPμ analyzed by immunoprecipitation with mAb 3D7 followed by immunoblotting (mAb 3G4). *Left panel*, wild-type RPTPμ from 3T3[FL] cells. *Right panel*, truncated RPTPμ from 3T3[XJ] cells.

lytic domain into proximity with its specific substrates. This, in turn, will then trigger intracellular signaling. In high-density cultures, we do detect decreased tyrosine phosphorylation of one or more protein(s) in the 110–130-kD region, whose identity is currently unknown (Fig. 6 *C*). However, it remains to be investigated whether this net tyrosine dephosphorylation is causally related to upregulation of RPTPμ.

In conclusion, we propose that RPTPμ functions as a receptor that signals homophilic cell–cell contact and thereby may regulate, either directly or indirectly, contact-mediated cellular responses such as growth inhibition, differentiation, and/or morphogenesis. As such, RPTPμ and related adhesive receptor PTPs may act in parallel, and perhaps in synergy, with other homophilic cell–cell adhesion molecules like the cadherins. Further understanding of the biological function(s) of RPTPμ awaits the identification and characterization of its physiological substrates.

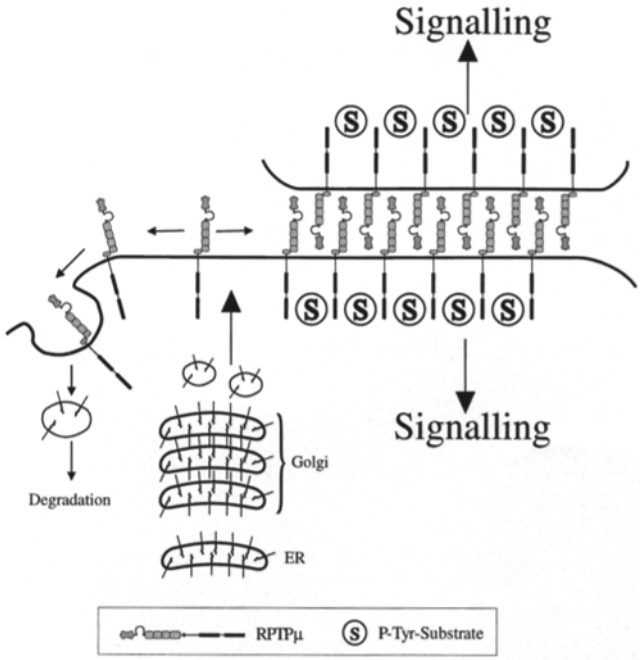

Figure 8. Proposed model of RPTPμ regulation by cell–cell contact. Cells that do not make contact with neighboring cells express low levels of RPTPμ on their cell surface due to rapid internalization. Cell–cell contact causes RPTPμ to be trapped at the cell surface through homophilic binding, which leads to local accumulation of RPTPμ at intercellular contact sites. Clustering of RPTPμ then triggers signaling. Ectodomain shedding has not been included in this figure. For details see Discussion.

We thank L. Oomen for assistance with confocal microscopy and E. Nooteboom for help with FACS® analysis.

This work was supported by the Dutch Cancer Society.

Received for publication 21 February 1995 and in revised form 5 May 1995.

References

Beckmann, G., and P. Bork. 1993. An adhesive domain detected in functionally diverse receptors. *Trends Biochem. Sci.* 18:40–41.

Brady-Kalnay, S. M., and N. K. Tonks. 1994. Identification of the homophilic binding site of receptor protein tyrosine phosphatase PTPμ. *J. Biol. Chem.* 269:28472–28477.

Brady-Kalnay, S. M., A. J. Flint, and N. K. Tonks. 1993. Homophilic binding of PTPμ, a receptor-type protein tyrosine phosphatase, can mediate cell–cell aggregation. *J. Cell Biol.* 122:961–972.

Burgoon, M., M. Grumet, V. Mauro, G. Edelman, and B. Cunningham. 1991. Structure of the chicken neuron-glia cell adhesion molecule, Ng-Cam: origin of the polypeptides and relation to the Ig superfamily. *J. Cell Biol.* 112:1017–1029.

Gebbink, M. F. B. G., I. van Etten, G. Hateboer, R. Suijkerbuijk, R. L. Beijersbergen, A. Geurts van Kessel, and W. H. Moolenaar. 1991. Cloning, expression and chromosomal localization of a new putative receptor-like protein tyrosine phosphatase. *FEBS (Fed. EUr. Biochem. Soc.) Lett.* 290:123–130.

Gebbink, M. F. B. G., G. C. M. Zondag, R. W. Wubbolts, R. L. Beijersbergen, I. van Etten, and W. H. Moolenaar (1993*a*). Cell-cell adhesion mediated by a receptor-like protein tyrosine phosphatase. *J. Biol. Chem.* 268:16101–16104.

Gebbink, M. F. B. G., M. H. G. Verheijen, G. C. M. Zondag, I. van Etten, and W. H. Moolenaar. 1993*b*. Purification and characterization of the cytoplasmic domain of human receptor-like protein tyrosine phosphatase RPTPμ. *Biochemistry.* 32:13516–13522.

Harlow, E., and D. Lane. 1988. Antibodies: A Laboratory Manual. Cold Spring Harbor Laboratory Press, Cold Spring Harbor, NY. 726 pp.

Jiang, Y.-P., H. Wang, P. D'Eustachio, J. M. Mussacchio, J. Schlessinger, and J. Sap. 1993. Cloning and characterization of R-PTP-κ, a new member of the receptor protein tyrosine phosphatase family with a proteolytically cleaved extracellular adhesion molecule-like extracellular region. *Mol. Cell. Biol.* 13: 2942–2952.

Livney, E., N. Reiss, E. Berent, A. Ullrich, and J. Schlessinger. 1987. An insertional mutant of epidermal growth factor receptor allows dissection of diverse receptor functions. *EMBO (Eur. Mol. Biol. Organ.) J.* 6:26669–26676.

Margolis, B., S. G. Rhee, S. Felder, M. Mervic, R. Lyall, A. Levitzki, A. Ullrich, A. Zilberstein, and J. Schlessinger. 1989. EGF induces tyrosine phosphoryla-

tion of phospholipase C-II: a potential mechanism for receptor signaling. *Cell* 57:1101–1107.

Miyazono, K., L. Claesson-Welsh, and C.-H. Heldin. 1988. Latent high molecular weight complex of transforming growth factor μ. *J. Biol. Chem.* 263: 6407–6415.

Östman, A., Q. Yang, and N. K. Tonks. 1994. Expression of DEP-1, a receptor-like protein-tyrosine-phosphatase, is enhanced with increased cell density. *Proc. Natl. Acad. Sci. USA.* 91:9680–9684.

Sap, J., Y.-P. Jiang, D. Friedlander, M. Grumet, and J. Schlessinger. 1994. Receptor tyrosine phosphatase R-PTP-κ mediates homophilic binding. *Mol. Cell. Biol.* 14:1–9.

Schaap, D., J. van der Wal, W. J. van Blitterswijk, R. L. van der Bend, and H. L. Ploegh. 1993. Diacylglycerol kinase is phosphorylated *in vivo* upon stimulation of the epidermal growth factor receptor and serine/threonine kinases, including protein kinase C-ε. *Biochem. J.* 289:875–881.

Serra-Pages, C., H. Saito, and M. Streuli. 1994. Mutational analysis of proprotein processing, subunit association and shedding of the LAR transmembrane protein tyrosine phosphatase. *J. Biol. Chem.* 269:23632–23641.

Smith, D. B. and K. S. Johnson. 1988. Single-step purification of polypeptides expressed in *Escherichia coli* as fusions with glutathion *S*-transferase. *Gene* 67:31–40.

Spivak, G., A. K. Ganesam, and P. C. Hanawalt. 1984. Enhanced transformation of human cells by UV-irradiated pSV2 plasmids. *Mol. Cell. Biol.* 4:1169–1171.

Streuli, M., N. X. Krueger, P. D. Ariniello, M. Tang, J. M. Munro, W. A. Blattler, D. A. Adler, C. M. Disteche, and H. Saito. 1992. Expression of the receptor-linked protein tyrosine phosphatase LAR: proteolytic cleavage and shedding of the CAM-like extracellular region. *EMBO (Eur. Mol. Biol. Organ.) J.* 11:897–907.

Walton, K. M., and J. E. Dixon. 1993. Protein tyrosine phosphatases. *Annu. Rev. Biochem.* 62:101–120.

Yu, Q., T. Lenardo, and R. A. Weinberg. 1992. The N-terminal and C-terminal domains of a receptor tyrosine phosphatase are associated by non-covalent linkage. *Oncogene* 7:1051–1057.

Zondag, G. C. M., G. Koningstein, Y.-P. Jiang, J. Sap, W. H. Moolenaar, and M. F. B. G. Gebbink. 1995. Homophilic interactions mediated by receptor tyrosine phosphatases μ and κ: a critical role for the novel extracellular MAM domain. *J. Biol. Chem.* 270:14247–14250.